Simulation of Contaminant Transport in Unconfined Coastal Aquifers

R E Volker, Q Zhang and D A Lockington
Department of Civil Engineering, The University of Queensland, Qld 4072, Australia

Abstract In coastal aquifers, seawater intrusion induces a freshwater-saltwater interface at the seaward end. This interface complicates the seaward boundary condition and affects the groundwater flow pattern in the region near the interface and consequently affects contaminant transport. Since seawater may have a different chemical composition and density from the contaminant discharged from surface waste disposal, the inclusion of seawater in numerical modelling will require a mathematical formulation coping with two species of contaminants, which will be computationally expensive especially for density-dependent flow and transport. Therefore, it will be instructive to investigate the consequence of simplifying the seaward boundary condition by neglecting the seawater density and its influence on numerical prediction of contaminant transport. This paper employs a two-dimensional variable density flow and transport model to investigate the transport of a dense contaminant plume in an unconfined coastal aquifer. Experimental results are also presented to show the contaminant plume in a freshwater-seawater flow system. Both the numerical and experimental results suggest that the neglect of the seawater interface does not affect noticeably the horizontal migration rate of the plume before it reaches the interface. However, the contaminant will travel further seaward and part of the solute mass will exit under the sea if the higher seawater density is not included. If the seawater density is included, the contaminant will travel upwards towards the beach along the freshwater-saltwater interface as shown experimentally. Neglect of seawater density, therefore, will result in an under-estimate of solute mass exiting around the coastline and a fictitious migration path under the seabed. If concerns are focused on the impact of contaminant on the littoral zone or the exit face at the beach, it will not be appropriate to neglect the seawater intrusion.

1. INTRODUCTION

The development of coastal resorts and coastal urban subdivisions has increased the incidence of groundwater contamination in the zone immediately adjacent to the shoreline. Contaminants tend to enter the groundwater system and travel seaward in the ambient groundwater flow. They not only pollute the groundwater, but also endanger the littoral zone. The understanding and modelling of contaminant transport in coastal aquifers is, therefore, vital to management of the coastal environment.

At the seaward boundary of coastal aquifers, seawater intrusion occurs and there will be a saltwater interface between the freshwater and the sea. The saltwater interface complicates the seaward boundary condition and affects the flow pattern and consequently contaminant transport. Little work has been done on contaminant transport in the area near the saltwater interface. The inclusion of the dense seawater may result in excessive computational effort. Because seawater is not likely to have the same chemical composition and density as that of the contaminant from surface sources, the model has to have the capability to handle two species of dense contaminants. This requirement not only complicates the mathematical formulation of the model, but also results in sometimes, unaffordable computation. It is useful, therefore, to compare the groundwater flow pattern with and without seawater intrusion and to explore the influence on contaminant transport. If the seawater density increase can be safely neglected, great computational savings will be made. Tidal fluctuations of seawater level are also present at the seaward boundary. They may affect the flow and mass transport conditions if they are significant. However, tidal fluctuations have not been included in the work presented here. The objective of this paper is to investigate the impact of the seawater intrusion on the pattern of plume migration in unconfined coastal aquifers.

The two-dimensional variable density flow and transport model, 2DFEMFAT [Cheng et al., 1998 and Yeh et al., 1994], is used in this simulation. Experimental results are presented for contaminant transport in the presence of seawater intrusion. Both approaches are used to demonstrate the influence of the dense seawater on the migration of contaminant plumes.

2. EXPERIMENTAL SETUP AND PROCEDURE

Laboratory experiments were performed in a flow tank 1650 mm long, 600 mm high and 100 mm wide (Figure 1). Glass beads were packed in the tank as a homogeneous porous medium. The glass beads have a median grain size of 0.725 mm. The saturated hydraulic conductivity of the glass beads is measured to be 4.0 mm/s. Salt (NaCl) solutions are used as the seawater and the contaminant source. The upstream freshwater head is maintained constant, while the mobile weir at the seawater end controls the seawater level. Surface contaminant is introduced through a source, 180 mm × 90 mm, located on the top of the flow tank at X_0=335 mm (Figure 1). The source contains 4 rows of needles at the bottom, through which contaminant is injected. Each row has 7 needles with a uniform spacing of 30 mm. The liquid level in the source is maintained constant by a weir so that a constant injection rate is generated through the experimental runs. The glass beads were packed 535 mm high at the freshwater end and 365 mm high at the sea end. The vertical to horizontal ratio of the sloping seaward boundary is 1:6.12. The slope is stable under the experimental conditions.

Figure 2 shows a steady-state freshwater-saltwater system in the porous medium. The flow system is for a constant freshwater head of 463 mm and a constant seawater level of 439 mm. The seawater density is 1025 g/L. There are three zones in the system: the freshwater zone, the diffusion zone and the seawater zone. In the freshwater zone, freshwater enters into the aquifer at the upstream end and exits mainly at face BC into the sea. The freshwater flow changes direction gradually from horizontal to upward when it approaches the saltwater interface CD. The salt concentration at face BC is the same as that of the outflowing water. In other words, the concentration gradient normal to boundary BC is zero. In the diffusion zone CD, the salt concentration ranges from that of seawater to that of freshwater. Some of the mixed fluid in the diffusion zone moves upward to the sea with the discharge of freshwater, which causes the seawater flow into the mixing zone to maintain a balance of solute mass and forms a slight circulation in the seawater zone (the shaded area). The steady-state diffusion zone in our experiment is as narrow as 40 mm reflecting the small longitudinal dispersivity of 0.65 mm of the medium.

The unsaturated zone above the measured water table AB has an average depth of 75 mm. Since the porous medium has a capillary fringe of approximately 110 mm, the unsaturated zone remains fairly wet in the experiment. As a consequence, the seepage face at the sloping boundary is not apparent. The steady-state flow system in Figure 2 was used as the initial condition before introducing the surface contaminant. The density of the surface contaminant is 1015.7 g/L. This value is in the range of the average TDS (total dissolved solids) (5,000 - 40,000 mg/L) in leachate from landfills [Freeze and Cherry, 1979], which approximately corresponds to densities in the range 1002 g/L to 1028 g/L. The density difference between the contaminant and the freshwater is 2.1%. The experimental results will be presented in the comparison with the numerical results. The solute concentration of contaminant plumes was interpreted from an image processing technique [Russ, 1992; Schincariol et al., 1993].

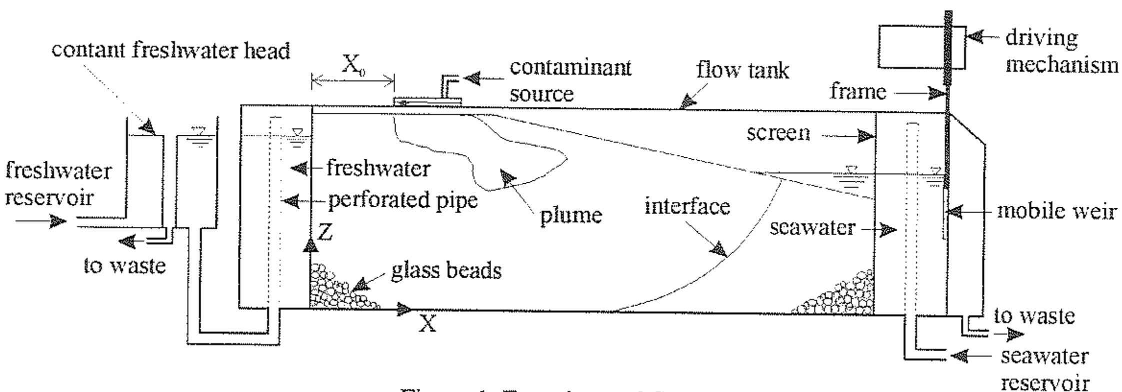

Figure 1. Experimental Setup.

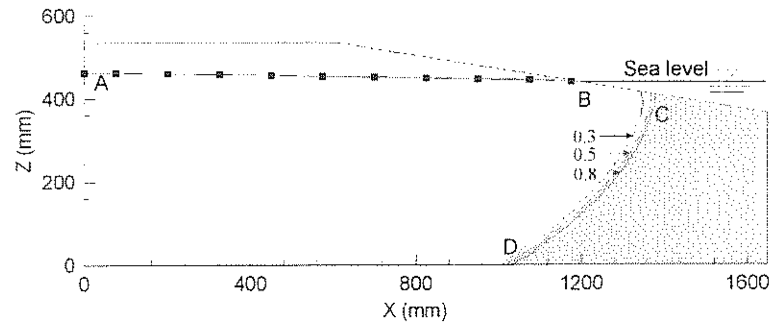

Figure 2. The freshwater-saltwater system in an unconfined coastal aquifer (AB is the measured free surface; BC is the outflowing face; CD is the diffusion zone shown by contours of relative salt concentrations of 0.3, 0.5 and 0.8; the shaded area is the seawater zone).

3. NUMERICAL MODELLING AND DISCUSSION

The computer model, 2DFEMFAT [Cheng et al. 1998] was used in this study. This is a density-dependent saturated-unsaturated finite-element model. The computer model was tested using the Henry seawater intrusion problem [Cheng et al., 1998]. However, the Henry seawater intrusion problem is a verification only for simulation of highly dispersed transition zones due to the large dispersion coefficient defined [Voss and Souza, 1987]. It does not check whether a model accounts for the density-driven flow accurately and whether the velocity is consistent. The Elder free convection problem [Elder, 1967] was suggested by Voss and Souza [1987] as a further testing example. The Elder problem can effectively check the ability of a model in simulating water flow driven purely by density differences of up to 20%. A coarse mesh of 44 × 25 elements and a finer mesh of 60 × 32 were used for the Elder problem. Both meshes produced satisfactory results showing the same number of convective flow circulations and the same direction (results not shown) as Elder's experimental results [Elder, 1967] and the results in Oldenburg and Pruess [1995]. SUTRA [Voss, 1984] failed to produce a central upwelling for the Elder problem at times of 10 and 20 years when the same mesh of 44 × 25 elements was used [Voss and Souza, 1987]. This indicates that the computer code 2DFEMFAT provides better accuracy for a relatively coarse mesh and hence it is employed in this study.

The model was then calibrated against the experimental result of Figure 2 using the measured physical parameters. The longitudinal dispersivity, α_L, of the porous medium is measured to be 0.65 mm from one-dimensional column experiments. Considering the small dispersivity of the medium, a quite fine mesh of 3840 quadrilateral elements with a total of 3969 nodes was adopted for the domain of Figure 2. This discretisation results in a grid Peclet number of 31.7 in the horizontal direction. The transverse dispersivity, α_T, is assumed to be half of α_L. The actual value is unknown and could be less than that. We used this value simply because, for a smaller value, a much finer mesh is required. According to the criterion in Voss and Souza [1987], the transverse spacing of the mesh is preferably to be no larger than $10\alpha_T$. For our discretisation, the vertical spacing of the mesh ranges from $23\alpha_T$ to $34\alpha_T$. A smaller transverse dispersivity will require a huge number of nodes and this was not attempted in this simulation.

Equivalent freshwater heads are imposed at the seaward boundary starting from point B (Figure 2), which is calculated as

$$H_f = Z + (H_s - Z)\cdot\frac{\rho_s}{\rho_f} \tag{1}$$

where, H_f (L) is the equivalent freshwater head; Z (L) is the Z-coordinate of a boundary node; H_s (L) is the seawater head; ρ_s (ML^{-3}) and ρ_f (ML^{-3}) are seawater and freshwater density, respectively (ρ_s=1025 g/L, ρ_f=995.1 g/L).

The boundary BC is an outflow face (C is the point where the 1.0 concentration contour meets the beach). The salt concentration at BC is equal to that of the outflowing fluid across it. Hence a zero salt concentration gradient is specified to allow free convective transport. A constant salt concentration of 1.0 is imposed at the seaward boundary from point C. The top surface is treated as a zero rainfall infiltration boundary. Under these conditions, the steady state freshwater-saltwater interface is shown in Figure 3(a). A comparison of the position of the 0.5 solute contour and the water table is shown in Figure 3(b). The results from 2DFEMFAT in terms of the width of the diffusion zone and the position of the 0.5 contour are in excellent agreement with the experimental ones, which implies the model can reproduce the experimental results and the parameters used may be appropriate.

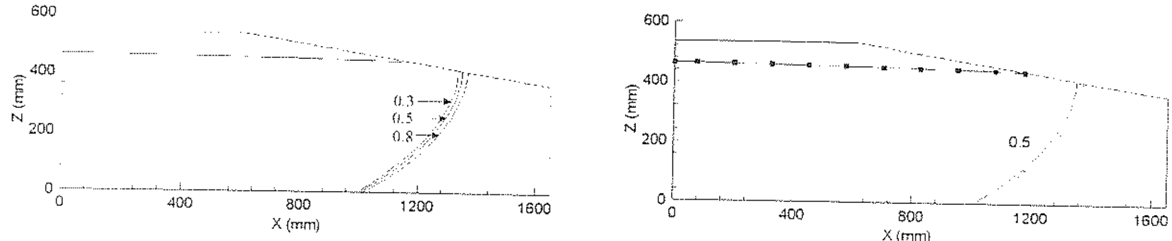

(a) steady state solution from 2DFEMFAT (b) comparison of 0.5 contours

Figure 3. Steady state solution from 2DFEMFAT (the dotted-line is the experimental result).

In the current work, the seaward boundary condition is simplified as a constant freshwater head by neglecting the seawater density so that seawater intrusion will not occur. A zero concentration gradient is specified along the seaward boundary to allow free convective transport of solute across the boundary when the contaminant reaches there. A Cauchy flow boundary condition in conjunction with a unit concentration is used to represent the contaminant source. The contaminant flux, 0.15 mm/s, at the surface is calculated from the total injection rate from the source area by assuming a uniform distribution across the width of the flow tank. A small time step of 30 seconds is used. Figure 4 shows the comparison of numerical and experimental results at different times up to 80 minutes and the numerical results for an extended simulation time to obtain the steady state solution at 190 minutes. Experiments terminated at 80 minutes when the contaminant joined the saltwater interface and hence the experimental results for longer times are not available.

The comparison of numerical model and experimental results in Figure 4 shows that in the horizontal direction, the outline of the plume from numerical modelling matches well with the experimental one before the contaminant reaches the saltwater interface. For management purposes, the seawater density may be neglected if we are only interested in the contaminant migration before it reaches the saltwater interface. However, the neglect of seawater density will allow the contaminant to travel all the way to the seaward boundary and exit both around the coastline and across the vertical boundary as shown in Figure 4(h). This is quite different from that when including the seawater density, in which case contaminant travels upward towards the coastline when it approaches the interface rather than travelling further seaward through the seawater wedge. The different migration and exit manner near the seaward end arises from the different flow patterns with and without seawater density change as shown in Figure 5. In Figure 5(a), groundwater exits only around the coastline. However, if the seawater density is not considered, groundwater exits both at the beach and at the vertical head-specified boundary, which results in the migration pattern in Figure 4 (h). The neglect of seawater density is likely to underestimate the solute mass exiting around the coastline and to suggest a fictitious migration path and exit points further seaward under the seabed. The neglect of seawater intrusion also excludes information on the contaminant movement after it enters into the saltwater diffusion zone, which, in reality, could be a few tens of meters or hundreds of meters wide [Todd, 1980]. Therefore, if concerns are on the impact of contaminant on the littoral zone or on the actual exit points and the exit solute concentration, seawater intrusion should be taken into account.

It is also noted that, in the experiments, the contaminant spreads faster in the vertical direction than the numerical prediction [Figure 4 (c), (d) and (e)]. This is because free convective instabilities occurred in the experiments for a density difference of 2.1%. These instabilities may occur as a dense contaminant travels in a less dense ambient water flow and under the perturbations of the heterogeneity of the natural medium [Schincariol et al., 1994]. The development and the behaviour of these instabilities are inherently unpredictable. The occurrence of instabilities may be related to some nondimensional parameters, such as the Rayleigh number [Wooding, 1963] or the modified Rayleigh number, R_a^* and π_l defined as [Oostrom et al., 1992a],

$$R_a^* = \frac{\pi_1 Q_L}{\varepsilon D_T W} \tag{2}$$

$$\pi_1 = \frac{K_{sat} \cdot \Delta\rho / \rho_0}{q_x} \tag{3}$$

where, K_{sat} [LT^{-1}] is the saturated hydraulic conductivity of the porous medium; $\Delta\rho/\rho_0$ is the relative density difference; q_x [LT^{-1}] is the horizontal Darcy flux of water flow; Q_L [L^3T^{-1}] is the leakage rate of contaminant from the source; ε is the porosity; D_T [L^2T^{-1}] is the transverse dispersion coefficient; W [L] is the width of the medium.

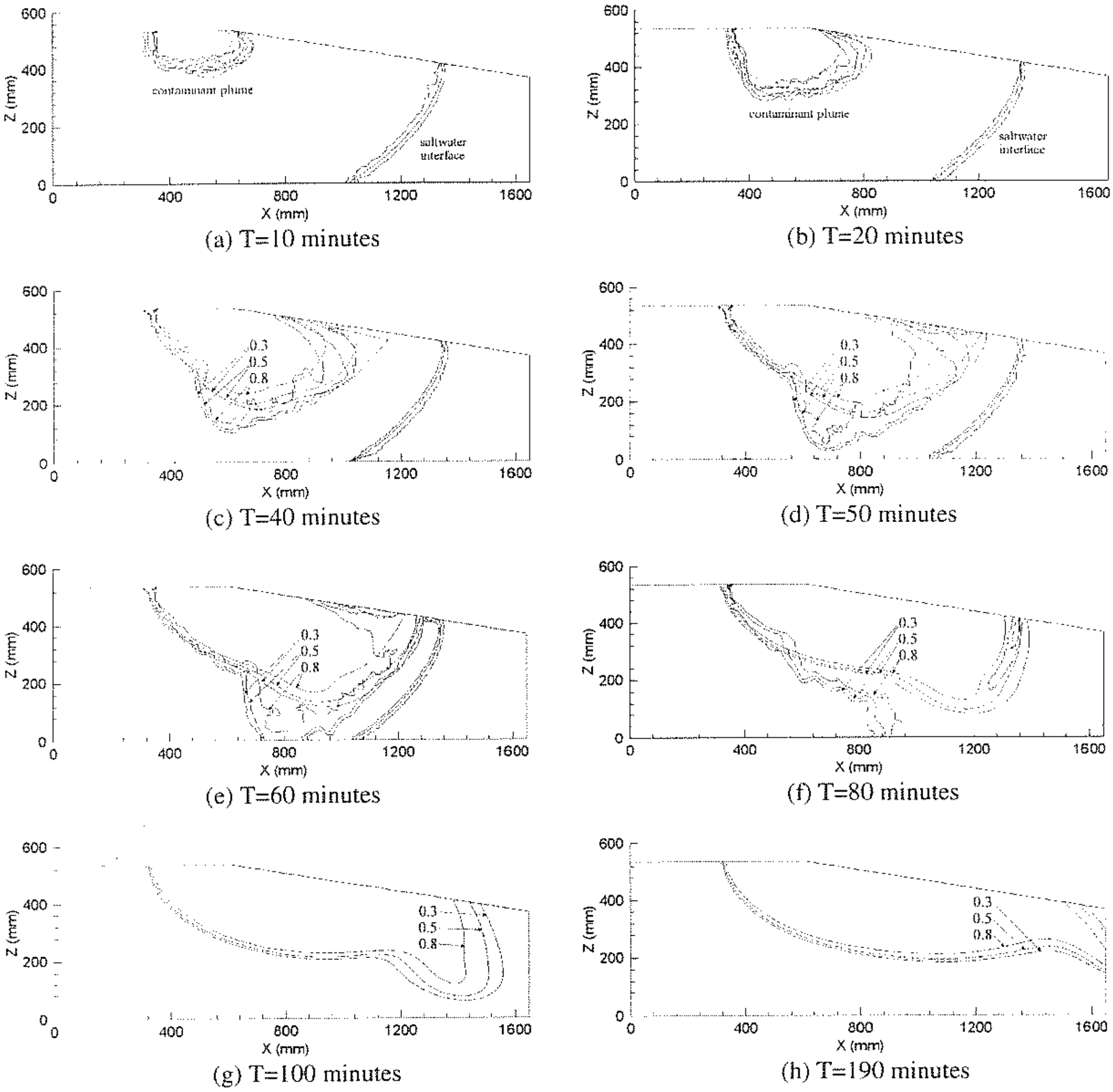

(a) T=10 minutes (b) T=20 minutes

(c) T=40 minutes (d) T=50 minutes

(e) T=60 minutes (f) T=80 minutes

(g) T=100 minutes (h) T=190 minutes

Figure 4. Contaminant migration from both numerical modelling and experimental results. The solid-line represents the experimental results with seawater intrusion; the dashed-line is for the numerical results without seawater density. The contours of relative solute concentrations of 0.3, 0.5 and 0.8 are plotted.

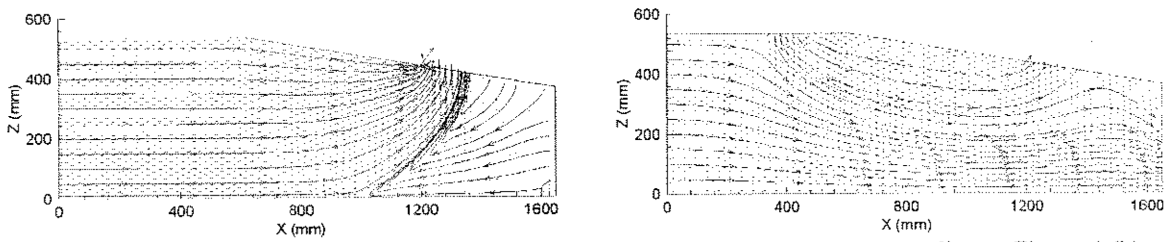

(a) flow pattern corresponding to Figure 2. (with seawater density)

(b) flow pattern corresponding to Figure 4 (h) (without seawater density)

Figure 5. Different flow patterns at the seaward boundary with or without seawater density.

The values of π_I and R_a^* for our experiment are calculated as 1.35 and 6432, respectively. Oostrom et al. [1992a] concluded that the transition from stable to unstable plumes occurs around π_I=0.3 or from a lower limit of R_a^*=150 to an upper limit of R_a^*= 250 or 750 depending upon the method of calculating D_T. According to these criteria, the value of π_I and R_a^* for our experiment suggests that the plume is unstable. In numerical modelling, the instabilities may not occur unless appropriate artificial disturbances or numerical errors are introduced [Schincariol et al., 1994]. The modelling and generating of the instabilities are beyond the scope of this paper. In our modelling, neither artificial disturbances nor numerical errors were introduced. Therefore, such instabilities are not observed in the numerical results.

4. CONCLUSIONS

Numerical simulations were performed to investigate the transport of a dense contaminant plume in an unconfined coastal aquifer. In modelling, the seaward boundary condition is simplified as a constant freshwater head by neglecting the seawater density. The numerical results were then compared with experimental results where the seawater density was included and consequently an intruded seawater wedge formed. It is found that before the contaminant reaches the saltwater interface, the numerical prediction matches well the experimental result in terms of travel rate of the plume in the horizontal direction. The experimental results show that the contaminant moves upward towards the coastline when it approaches the saltwater interface and then exits around the coastline. It does not travel through the intruded seawater and exit at some place further seaward. When the seawater density is not considered, a different flow pattern results. In this flow pattern, the contaminant travels further seaward and part of the solute exits at the seaward boundary under the seabed. Therefore, the exclusion of seawater intrusion in numerical modelling will result in an underestimate of solute mass exiting at the coastal beach and an unrealistic migration path under the seabed. If more detailed and accurate information is needed on the impact of contaminant on the littoral zone or on the actual exit points and the exit solute concentration, seawater intrusion will need to be included.

Instabilities occur when a dense contaminant is present in a less dense groundwater flow. Artificial disturbances are needed to generate the instabilities in numerical modelling and this was not attempted in this work.

Acknowledgments

Financial support was provided through the Cooperative Research Centre for Ecological Sustainability of the Great Barrier Reef.

References

Cheng, Jing-Ru, Robert O. Strobl, Gour-Tsyh Yeh, Hsin-Chi Lin, and Woo Hee Choi, Modelling of 2D density-dependent flow and transport in the subsurface, *J. of Hydrologic Engineering*, 3(4), 248-257, 1998.

Elder, J. W., Transient convection in a porous medium, *J. of Fluid Mech.*, 27(3), 609-623, 1967.

Freeze, R. Allan, and John A. Cherry, Groundwater, Prentice-Hall, Inc., Englewood Cliffs, N. J., 1979.

Oldenburg, Curtis M., and Karsten Pruess, Dispersive transport dynamics in a strongly coupled groundwater-brine system, *Water Resour. Res.*, 31(2), 289-302, 1995.

Oostrom, M., J. S. Hayworth, J. H. Dane, and O. Guven, Behavior of dense aqueous phase leachate plumes in homogeneous porous media, *Water Resour. Res.*, 28(8), 2123-2134, 1992a.

Oostrom, M., J. H. Dane, O. Guven, and J. S. Hayworth, Experimental investigation of dense solute plumes in an unconfined aquifer model, *Water Resour. Res.*, 28(9), 2315-2326, 1992b.

Russ, John C., The image processing handbook, CRC Press, Inc., 1992.

Schincariol, Robert A., Edward E. Herderick, and Franklin W. Schwartz, On the application of image analysis to determine concentration distributions in laboratory experiments, *J. of Contaminant Hydrology*, 12, 197-215, 1993.

Schincariol, Robert A., Franklin W. Schwartz, and Carl A. Mendoza, On the generation of instabilities in variable density flow, *Water Resour. Res.*, 30(4), 913-927, 1994.

Todd, D. K., Groundwater Hydrology, John Wiley & Sons, 1980.

Voss, Clifford I., SUTRA: A finite-element simulation model for saturated-unsaturated fluid-density-dependent groundwater flow with energy transport or chemically-reactive single-species solute transport, *U.S. Geol. Surv. Water Resour. Invest. Rep., 84-4369*, 409 pp., 1984.

Voss, Clifford I., and William R. Souza, Variable density flow and solute transport simulation of regional aquifers containing a narrow freshwater-saltwater transition zone, *Water Resour. Res.*, 23(10), 1851-1866, 1987.

Wooding, R. A., Convection in a saturated porous medium at large Rayleigh number or Peclet number, *J. of Fluid Mech.*, 15, 527-544, 1963.

Yeh, G. T., Strobl, R. O. and Cheng, J. R., 1994. 2DFEMFAT: A Two-dimensional Finite Element Model of Density-dependent Flow and Transport Through Saturated-unsaturated Porous Media: version 2.0. Department of Civil and Environmental Engineering, The Pennsylvania State University, University Park, PA 16802.